Seismic response control of buildings using mechanical linkages with passive dampers

Y. Miyazu & A. Itou

Department of Architecture, Hiroshima University, Higashi-Hiroshima, Japan.

S. Soda

Department of Architecture, Waseda University, Tokyo, Japan.

M. Ohsaki

Department of Architecture and Architectural Engineering, Kyoto University, Kyoto, Japan.

ABSTRACT: A mechanical linkage with passive dampers (MLD) that prevents a soft story mechanism of a mid- and low-rise building is proposed. The proposed device consists of a stiff frame, a passive damper, and rotational friction devices, and is mounted on the adjoining two stories. The stiff frame and the passive damper work to equalize the story deformation of the two stories, while the rotational friction device enhances the energy dissipation performance of a building. The mechanical model of the MLD is formulated as multi-mass shear system, and then prediction formula for the required force of the MLD is derived using the mechanical model. The validity of the prediction formula is verified through time-history response analysis. Shake table tests on scaled three-story steel frame and a numerical study for the test frame are carried out to show that the MLD realize uniform story deformation of all the stories and decreases the seismic response owing to the rotational friction device.

1 INTRODUCTION

In resent years, many earthquake ground motions that exceed the intensity of design ground motions have been recorded. Under such severe ground motions, many mid- and low-rise buildings have collapsed due mainly to concentration of deformation at one or a few stories. Collapse in a few stories, so-called soft story mechanism, should be prevented because it directly causes loss of human life. However, it is difficult to control the damage distribution of a building under strong ground motions that lead the structure to inelastic deformation, because of *P-Δ* effects and material non-linearity of structural members.

Various approaches have been presented to prevent the soft story mechanism. Alavi and Krawinkler (2004) demonstrated that strengthening with walls hinged at the base is effective in equalizing story deformations of a multi-story building. Qu et al. (2012) proposed to install passive energy dissipation devices between the hinged wall and the building to enhance the energy dissipation performance. Soda and Yasuda (2007) developed linked oil dampers that utilize hydraulic mechanical linkage, and Miyazu and Soda (2013) investigated its effectiveness on avoiding damage concentration and dissipating seismic input energy. Many other researches aiming at similar effects have been presented by Akiyama and Takahashi (1984), Lai and Mahin (2014), Midorikawa et al. (2010), Takeuchi et al. (2014), Gelagoti et al. (2012), and Qu et al. (2014).

In a previous study by Miyazu et al. (2015a, 2015b), an external device using mechanical linkage is proposed to make story deformation of the building uniform, and its effectiveness on seismic response reduction is demonstrated through numerical and experimental studies. In this study, we propose installation of a rotational friction device in the mechanical linkage to enhance the energy dissipation performance. The mechanical model of the proposed device is formulated as multi-mass shear system. A prediction formula for the force of the device required to equalize the story deformations is derived using the mechanical model, and its accuracy is verified through time-history analysis. A numerical study of a three-story steel frame is carried out to demonstrate the effect of the proposed device on seismic response reduction.

2 MECHANICAL LINKAGES WITH PASSIVE DAMPERS

We first illustrate a mechanical linkage with passive dampers (MLD), proposed in this study, and then formulate the mechanical model of the MLD as multi-mass shear system. Figure 1 shows the schematic of a building with the MLD. A stiff frame is mounted on the ith and the $i-1$th floors, and a damper is installed between the $i+1$th floor and the point of the stiff frame. In the previous study by Miyazu et al. (2015a), the stiff frame is connected to the main structure by hinges; however, in this study, the rotational friction device is installed into the connection to enhance the energy dissipation performance.

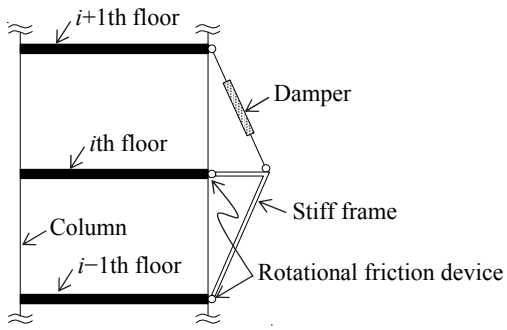

Figure 1. Schematic of a building with the MLD

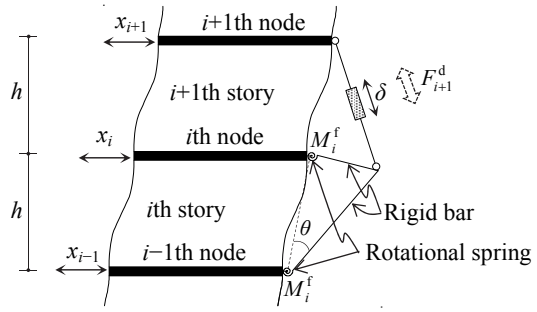

Figure 2. A mechanical model of a building with the MLD

The mechanical model of the MLD is illustrated in Figure 2. Let x_i, θ, and h denote the displacement of the ith node, the angle of the stiff frame, and the height of a story, respectively. The stiff frame is modeled using rigid bars for simplicity. The rotational friction device is represented by a rotational spring located at the end of the rigid bar. Under assumption of small deformation, the elongation δ of the damper is evaluated by

$$\begin{aligned}\delta &= (x_i - x_{i-1})\tan\theta\cos\theta - (x_{i+1} - x_i)\sin\theta \\ &= [(x_i - x_{i-1}) - (x_{i+1} - x_i)]\sin\theta\end{aligned} \tag{1}$$

The first term and the second term of the right-hand side are the elongations due to the story deformation of the ith and the $i+1$th story, respectively. The elongation of the damper is proportional to the difference between the story deformation of the ith story and that of the $i+1$th story; therefore, the damper works to equalize the story deformations of the two stories.

Let F^{d}_{i+1} and M_i^{f} denote the axial force of the damper and the moment of the rotational spring, respectively. Then, the forces F_{i-1}, F_i, and F_{i+1}, acting on each node from the MLD, are evaluated as follows by considering equilibrium of force.

$$\begin{Bmatrix} F_{i-1} \\ F_i \\ F_{i+1} \end{Bmatrix} = \sin\theta \begin{Bmatrix} F^{\mathrm{d}}_{i+1} \\ -2F^{\mathrm{d}}_{i+1} \\ F^{\mathrm{d}}_{i+1} \end{Bmatrix} + \frac{2}{h} \begin{Bmatrix} M_i^{\mathrm{f}} \\ -M_i^{\mathrm{f}} \\ 0 \end{Bmatrix} \tag{2}$$

3 PREDICTION OF REQUIRED FORCE OF DAMPERS

3.1 Derivation of prediction formula

Using the mechanical model obtained in the previous section, we derive the prediction formula for the required force of the damper. Here, a n-story building that has the MLDs in all the stories, as illustrated in Figure 3, is used as a structural model. Let m_i and Q_i denote the mass of the ith node and the story shear force of the ith story, respectively. The relative acceleration of the ith node and the ground acceleration are represented by $\ddot{x}_i$ and $\ddot{x}_0$, respectively; then, the equilibrium of force at the ith node is formulated as follows:

$$m_i\left(\ddot{x}_i+\ddot{x}_0\right)+\left(Q_i-Q_{i+1}\right)+\left(2F_{i+1}^{\mathrm{d}}-F_i^{\mathrm{d}}-F_{i+2}^{\mathrm{d}}\right)\sin\theta+\frac{2}{h}\left(M_i^{\mathrm{f}}-M_{i+1}^{\mathrm{f}}\right)=0 \tag{3}$$

where F_1^{d}, F_{n+1}^{d}, F_{n+2}^{d}, M_n^{f}, M_{n+1}^{f}, and Q_{n+1} are equal to zero. This equation is obtained by adding the fourth term of the left-hand side to the equation formulated in the previous study (Miyazu 2015a). Here, we assume that the story deformations of all the stories become perfectly equal to each other by installing the MLDs, then the relative acceleration of the *i*th node is given as

$$\ddot{x}_i=i\ddot{x}_1 \tag{4}$$

Equation 3 after substituting Equation 4 becomes

$$im_i\ddot{x}_1+\left(2F_{i+1}^{\mathrm{d}}-F_i^{\mathrm{d}}-F_{i+2}^{\mathrm{d}}\right)\sin\theta=Q_{i+1}-Q_i+\frac{2}{h}\left(M_{i+1}^{\mathrm{f}}-M_i^{\mathrm{f}}\right)-m\ddot{x}_0 \tag{5}$$

In the same manner, the equilibrium of force at all nodes are obtained as follows:

$$\mathbf{A}\mathbf{F}^{\mathrm{d}}=\mathbf{Q}-\mathbf{M}\mathbf{1}\ddot{x}_0 \tag{6}$$

where

$$\mathbf{A}=\left[\begin{array}{cccccc|c} 2 & -1 & & & & 0 & m_1 \\ -1 & 2 & -1 & & & & 2m_2 \\ & & \ddots & & & & \vdots \\ & & -1 & 2 & -1 & & (n-2)m_{n-2} \\ & & & -1 & 2 & & (n-1)m_{n-1} \\ 0 & & & & -1 & & nm_n \end{array}\right],\quad \mathbf{F}^{\mathrm{d}}=\begin{Bmatrix} F_2^{\mathrm{d}}\sin\theta \\ F_3^{\mathrm{d}}\sin\theta \\ \vdots \\ F_{n-1}^{\mathrm{d}}\sin\theta \\ F_n^{\mathrm{d}}\sin\theta \\ \ddot{x}_1 \end{Bmatrix},\quad \mathbf{1}=\begin{Bmatrix} 1 \\ 1 \\ \vdots \\ 1 \\ 1 \\ 1 \end{Bmatrix}$$

$$\mathbf{Q}=\begin{Bmatrix} Q_2-Q_1+2(M_2^{\mathrm{f}}-M_1^{\mathrm{f}})/h \\ Q_3-Q_2+2(M_3^{\mathrm{f}}-M_2^{\mathrm{f}})/h \\ \vdots \\ Q_{n-1}-Q_{n-2}+2(M_{n-1}^{\mathrm{f}}-M_{n-2}^{\mathrm{f}})/h \\ Q_n-Q_{n-1}+2(M_n^{\mathrm{f}}-M_{n-1}^{\mathrm{f}})/h \\ -Q_n \end{Bmatrix},\quad \mathbf{M}=\begin{bmatrix} m_1 & & & & & 0 \\ & m_2 & & & & \\ & & \ddots & & & \\ & & & m_{n-2} & & \\ & & & & m_{n-1} & \\ 0 & & & & & m_n \end{bmatrix}$$

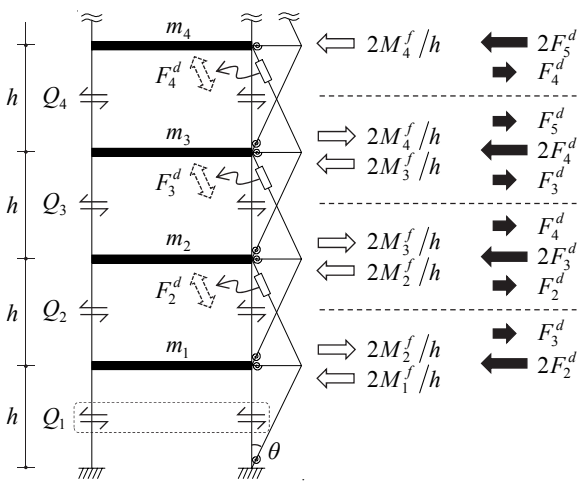

Figure 3. A building model with MLDs; ⇨: force by the friction device, ➡:force by the MLD

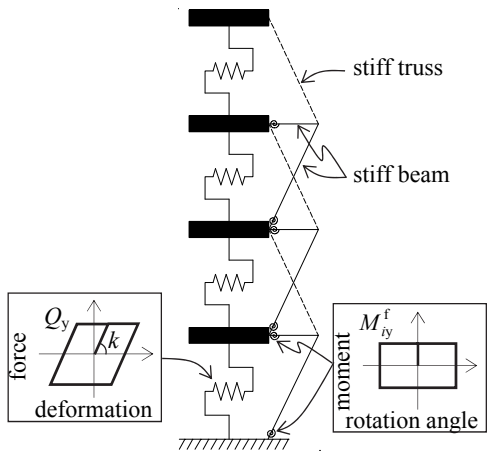

Figure 4. A model for time-history analysis

The damper forces are obtained by pre-multiplying both sides of Equation 6 by $\mathbf{A}^{-1}$:

$$\mathbf{F}^{\mathrm{d}} = \mathbf{A}^{-1}\left(\mathbf{Q} - \mathbf{M1}\ddot{x}_0\right) \tag{7}$$

Here, we assume that the damper force becomes the maximum when the ground motion takes its maximum absolute value $|\ddot{x}_0|_{\max}$ and the story shear forces have their maximum absolute values. This condition would be easy to occur when the force-deformation relation of the story shows the elastoplastic characteristic. Then, the required force $F^{\mathrm{d}}_{i\mathrm{lim}}$ of the damper can be predicted by

$$\mathbf{F}^{\mathrm{d}}_{\mathrm{lim}} = \max\left(\left|\frac{1}{\sin\theta}\mathbf{A}^{-1}\left(\mathbf{Q}_{\max} - \mathbf{M1}\left|\ddot{x}_0\right|_{\max}\right)\right|,\ \left|\frac{1}{\sin\theta}\mathbf{A}^{-1}\left(\mathbf{Q}_{\min} - \mathbf{M1}\left|\ddot{x}_0\right|_{\max}\right)\right|\right) \tag{8}$$

where

$$\mathbf{F}^{\mathrm{d}}_{\mathrm{lim}} = \begin{Bmatrix} F^{\mathrm{d}}_{2\mathrm{lim}} \\ F^{\mathrm{d}}_{3\mathrm{lim}} \\ \vdots \\ F^{\mathrm{d}}_{(n-1)\mathrm{lim}} \\ F^{\mathrm{d}}_{n\mathrm{lim}} \\ \ddot{x}_1/\sin\theta \end{Bmatrix} \qquad \mathbf{Q}_{\max} = \begin{Bmatrix} Q_{2\max} - Q_{1\max} + 2(M^{\mathrm{f}}_{2\max} - M^{\mathrm{f}}_{1\max})/h \\ Q_{3\max} - Q_{2\max} + 2(M^{\mathrm{f}}_{3\max} - M^{\mathrm{f}}_{2\max})/h \\ \vdots \\ Q_{(n-1)\max} - Q_{(n-2)\max} + 2(M^{\mathrm{f}}_{(n-1)\max} - M^{\mathrm{f}}_{(n-2)\max})/h \\ Q_{n\max} - Q_{(n-1)\max} + 2(M^{\mathrm{f}}_{n\max} - M^{\mathrm{f}}_{(n-1)\max})/h \\ -Q_{n\max} \end{Bmatrix}$$

The values of $Q_{i\max}$ and $M^{\mathrm{f}}_{i\max}$ correspond to the maximum story shear force of the ith story and the maximum moment of the rotational friction device of the ith story, respectively. Vector $\mathbf{Q}_{\min}$ is given by multiplying $\mathbf{Q}_{\max}$ by −1.

3.2 Verification of prediction formula

Time-history analyses are carried out to verify the prediction formula derived in the previous section. A four-story steel building model with the MLDs, used in the analysis, is illustrated in Figure 4. The main structure is modeled as multi-mass shear system, and the MLD is modeled using beam, truss, and rotational spring elements. The story height h is 3 m in all the stories.

The mass of 50,000 kg is attached at each node of the main structure. The hysteresis characteristic of the story is represented by an elastoplastic spring as illustrated in Figure 4. All the stories have the same yield strength Q_{y} and initial stiffness k. The stiffness of 1.818×10^8 N/m is assigned to the spring so that the natural period of the 1st mode of the main structure corresponds to 0.30 s. The yield strength Q_{y} is 5.88×10^5 N, which corresponds to 30 % of the total weight of the main structure.

The stiff frame of the MLD consists of two stiff beams that have a large cross-sectional area and a large second moment of area. The rotational friction device is modeled as a rotational elastoplastic spring with high initial stiffness, and is located at the end of the beam. The damper is represented by a truss element with a large cross-sectional area.

In the time-history analysis, the yield moment $M^{\mathrm{f}}_{i\mathrm{y}}$ of the rotational spring at each story is chosen as a parameter. The value of $M^{\mathrm{f}}_{i\mathrm{y}}$ is selected from 8.820×10^4, 2.646×10^5, and 4.410×10^5 (N·m), which correspond to 10 %, 30 %, and 50 %, respectively, of the value of ($h \times Q_{\mathrm{y}}$ / 2); therefore, the number of models to be calculated is 3^3 = 27. The NS component of 1995 JMA Kobe ground acceleration, which has the maximum value of 8.206 m/s^2, is used as input acceleration. The damping factor is defined as Rayleigh damping using the current tangent stiffness matrix, where the damping factors of the 1st and the 2nd modes are 0.02. Note that the natural periods of the 1st and the 2nd modes are 0.30 s and 0.10 s, respectively. The frame analysis software OpenSees (McKenna 2000) is used for the analysis.

Figure 5 shows the ratio of the maximum force of the damper obtained by the analysis to $F^{\mathrm{d}}_{i\mathrm{lim}}$ evaluated by Equation 8. The model that have $M^{\mathrm{f}}_{1\mathrm{y}}$ = 0.1 × ($h \times Q_{\mathrm{y}}$ / 2), $M^{\mathrm{f}}_{2\mathrm{y}}$ = 0.3 × ($h \times Q_{\mathrm{y}}$ / 2), and $M^{\mathrm{f}}_{3\mathrm{y}}$ = 0.5 × ($h \times Q_{\mathrm{y}}$ / 2) is named 10-30-50. It is found that the Equation 8 precisely evaluate the

required force of the damper. Note that all the stories reach the yield strength Q_y.

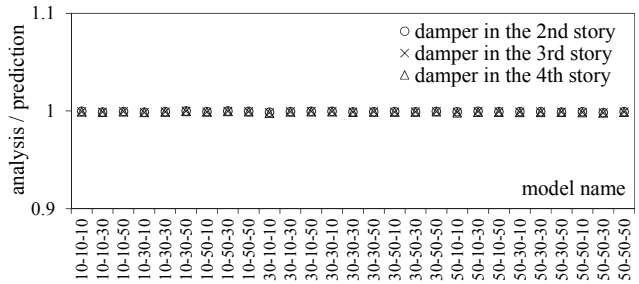

Figure 5. Ratio of the maximum force of the dampers obtained by the analysis to the predicted value $F^{\mathrm{d}}_{i\mathrm{lim}}$

4 NUMERICAL STUDY TO CONFIRM SHAKE TABLE TESTS

In this section, we first summarize the result of shake table tests on scaled three-story steel frames with the MLDs that don't have the rotational friction device (Miyazu 2015b), and then carry out time-history analyses to confirm the effectiveness of installing the rotational friction device.

4.1 Details of test frames

The photograph of the test frame without the MLD is shown in Figure 6. The height h of a story is 359 mm, and the width of the floor is 600 mm. Flat bars with 3 mm thickness and 25 mm width are used as columns. The ends of the column are fixed to the floors using steel angles of 65×65×6 (mm). The mass of the 1st, the 2nd, and the 3rd floors including columns are 41.0, 40.9, and 31.8 (kg), respectively. The natural period of the 1st mode is 0.50 s, and the yield strength Q_y of the story is 746 N, which corresponds to about 67 % of the total weight of the test frame. Shaking direction is one direction shown in a red arrow in Figure 6.

The MLDs are mounted on all the stories as illustrated in Figure 7. Figure 8 shows the photograph of two MLDs installed in the 2nd and the 3rd stories in parallel. The stiff frame of the MLD is composed of two steel angles of 25×25×3 (mm) that are connected to the floors using rod end bearings. Note that the rotational friction device is not installed at the end of the steel angle in this test. The two stiff frames in the same story are connected each other using two flat bars of 25×3 (mm) to constrain the out-of-plane deformation of the MLDs during shaking tests.

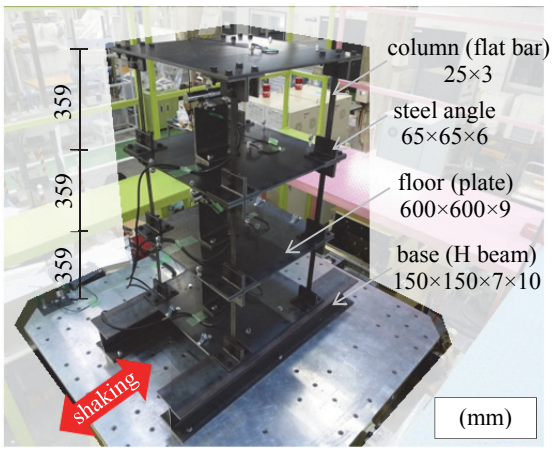

Figure 6. Photograph of the test frame without MLDs

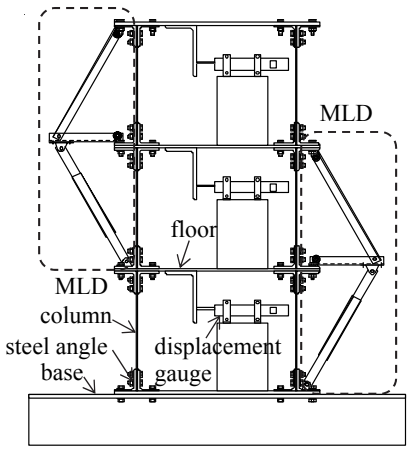

Figure 7. The test frame with MLDs

Two types of dampers, a viscoelastic damper (VED) and a friction type damper (FD), as illustrated in Figure 9, are used in this test. The viscoelastic damper consists of two flat bars and butyl rubber whose thickness and area are 3 mm and 2500 mm^2, respectively. In the friction type damper, neodymium magnets are utilized to generate friction force between the magnets and a polypropylene sheet bonded with the flat bar. The force-deformation relations of the dampers under gradual increasing sinusoidal excitation with 2 Hz are shown in Figure 10. It is seen that both dampers show stable hysteresis loops.

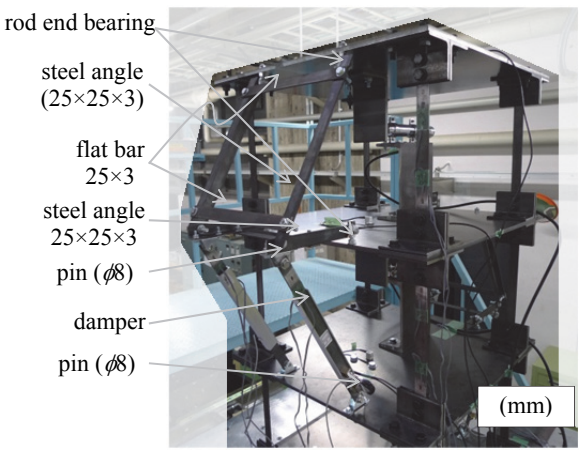

Figure 8. Photograph of the MLDs

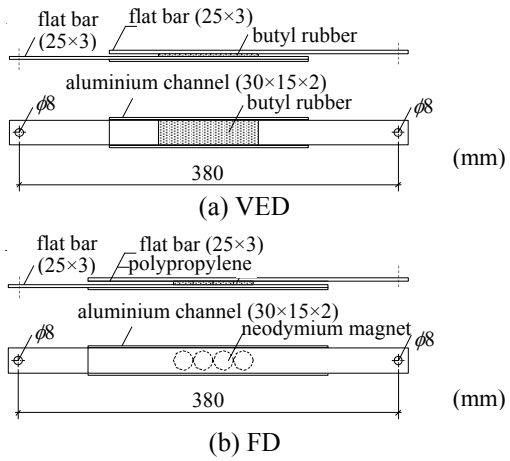

Figure 9. Details of two types of dampers

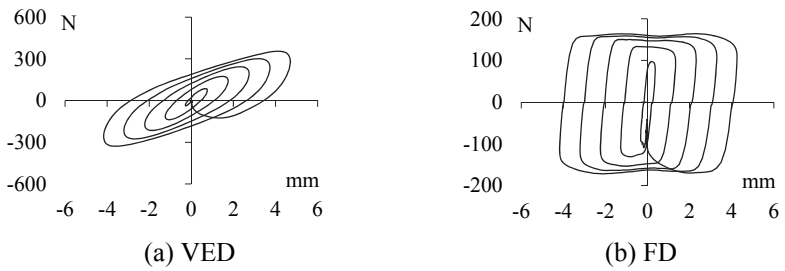

Figure 10. Force-deformation relations of the dampers under gradual increasing sinusoidal excitation with 2 Hz

4.2 **Response under earthquake excitation**

The frame with/without the MLDs are tested using a series of the NS component of the 1995 JMA Kobe ground motions normalized to 10 %, 20 %, 30 %, and 40 % of the original record. Figure 11 shows the relation between the maximum ground acceleration and the maximum story deformation in solid lines. It is noticed that installation of the MLD leads to smaller differences in the story deformations compared to the frame without the MLD, and reduces the maximum story deformation of the 1st story. Especially under the 40 % ground motion, the frame without the MLD shows soft story mechanism, while the MLD successfully prevents the damage concentration.

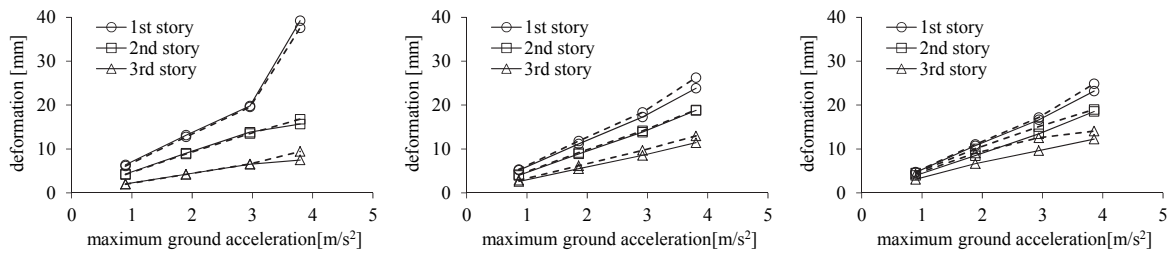

(a) Without MLD (b) With MLD (VED) (c) With MLD (FD)

Figure 11. Relation between the maximum ground motion and the maximum story deformation; solid line: experimental, dashed line: numerical

The force-deformation relations of the dampers under the 40 % ground motion are shown in Figure 12. The required force of the dampers evaluated by Equation 8, under the 40 % ground motion with the maximum acceleration of 3.79 m/s^2, are 637 N in the 1st story and 713 N in the 2nd story; therefore, it is noticed that the maximum forces of the dampers shown in Figure 12 are less than the predicted values. In the next section, time-history analyses are carried out to investigate the seismic response of the frame with enough amounts of dampers and the rotational friction devices.

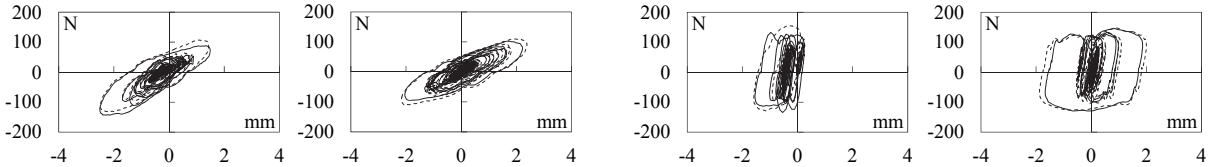

(a) VED; left: 1st story, right: 2nd story (b) FD; left: 1st story, right: 2nd story

Figure 12. Force-deformation relations of the dampers under 40 % JMA Kobe ground motion

4.3 Time-history analysis

We first verify the validity of a numerical model through comparing numerical and experimental results. The test frame is modeled as a two dimensional structure as shown in Figure 13. Rotational elastoplastic springs are installed at the ends of the column to consider the yielding of the column. The mechanical property of the VED is simulated by a generalized Maxwell model as shown in Figure 14(a). The FD is modeled using a friction element, a non-linear dashpot, and a linear spring, as shown in Figure 14(b), in order to simulate velocity dependency and initial stiffness as seen in Figure 10(b). P-Δ effects are considered in the analysis. The story deformation obtained by the time-history analysis is compared with experimental results in Figure 11. It is noticed that the numerical results shown in dashed lines agree well with the experimental results.

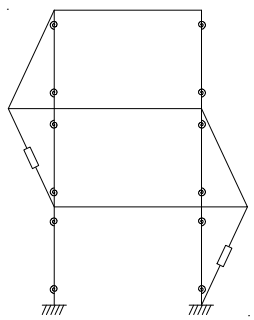

Figure 13. A model of the test frame without the rotational friction devices

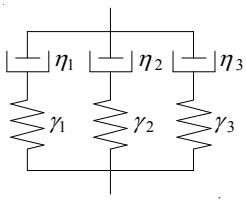

η_1	70.5	N·s/mm
η_2	4.0	
η_3	1.4	
γ_1	23.3	N/mm
γ_2	27.2	
γ_3	128.0	

*per damper

η: coefficient of viscosity
γ: coefficient of elasticity

(a) VED

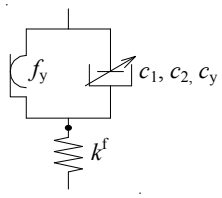

f_y	80	N
c_1	3.1	N·s/mm
c_2	0.42	N·s/mm
c_y	64.9	N
k^f	500	N/mm

*per damper

f_y: frictional force
c_1, c_2: initial and second damping coefficient
c_y: yield force
k^f: stiffness

(b) FD

Figure 14. Mechanical models of the dampers

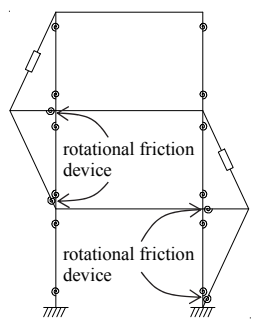

Figure 15. A model of the test frame with rotational friction devices

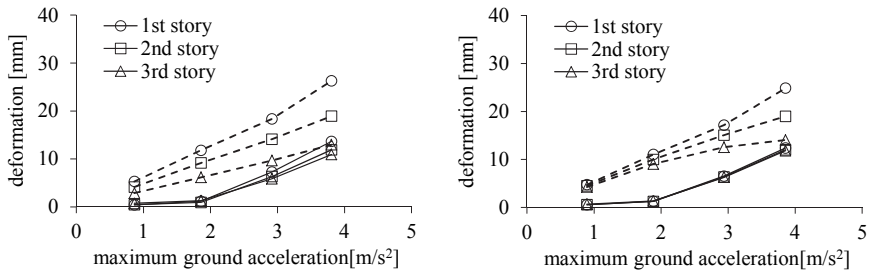

(a) With MLD (VED) (b) With MLD (FD)

Figure 16. Relation between the maximum ground motion and the maximum story deformation; solid line: with the rotational friction devices, dashed line: without the rotational friction devices

Figure 15 shows the model with the rotational friction devices. In a real structure, the rotational friction device is to be composed of friction pads and disc springs. In figure 15, the MLDs are mounted upside-down compared to the test frame, since the deformation in the lower story tends to be large as seen from Figure 11. The yield moment of 2.68×10^4 N·mm, which corresponds to 20 % of the value of ($h \times Q_y$ / 2), is assigned to the rotational friction device. The required forces of the damper in the 2nd and the 3rd stories are 605 and 598 (N), respectively, by Equation 8. Here, we simply increase the amount of the damper so that the maximum forces of the dampers shown in Figure 12 correspond

to the predicted required forces. Figure 16 shows the maximum story deformation under the same ground motions used in the shake table test. It is seen that the story deformations are almost the same in all the stories, and the maximum deformation successfully decreases owing to the rotational friction devices.

5 CONCLUSIONS

A new seismic device has been proposed for preventing a building from collapsing at a few stories under severe earthquake excitations. The frame with the proposed device exhibits uniform story deformation, and reduces the seismic response by dissipating input energy through the rotational friction devices. The force of the damper required to equalize the deformation of all the stories can be predicted by the proposed formula.

ACKNOWLEDGMENT

This research is supported by JSPS KAKENHI Grant Number 26820235 (Yuji Miyazu) and 26289195 (Satsuya Soda). The shake table test in section 4 is conducted at Waseda University.

REFERENCES:

Akiyama, H. & Takahashi, M. 1984. D_s-Values for Damage-Dispersing Type Multi-Story Frames. *Journal of Structural and Construction Engineering*. 341. 54-61 (in Japanese).

Alavi, B. & Krawinkler, H. 2004. Strengthening of moment-resisting frame structures against near-fault ground motion effects. *Earthquake Engineering and Structural Dynamics*. 33. 707-722.

Gelagoti, F., Kourkoulis, R., et al. 2012. Rocking isolation of low-rise frame structures founded on isolated footings. *Earthquake Engineering and Structural Dynamics*. 41. 1177-1197.

Lai, J.W. & Mahin, S.A. 2014. Strongback System: A Way to Reduce Damage Concentration in Steel-Braced Frames. *Journal of Structural Engineering*. 10.1061/(ASCE)ST.1943-541X.0001198 , 04014223.

McKenna, F., Fenves, G. L., Scott, M. H., and Jeremic, B. 2000. Open System for Earthquake Engineering Simulation (OpenSees). Pacific Earthquake Engineering Research Center, University of California, Berkeley, CA.

Midorikawa, M., Takeuchi, T., et al. 2010. Seismic Performance of Controlled Rocking Frames with Shear Fuse and PT Wire Anchorage -Shaking table tests on controlled rocking steel frames using multipurpose inertial mass system: Part I-. *Journal of Structural and Construction Engineering*. 75(654). 1547-1556. (in Japanese)

Miyazu, Y. & Soda, S. 2013. Seismic Response Control by Linked Oil Dampers. *13th World Conference on Seismic Isolation; Proc. Intern. Symp., Sendai, 24-27 September 2013*.

Miyazu, Y. & Soda, S. 2015a. Seismic Response Control of Mid- and Low-rise Buildings using External Story Deflection Control devices. *Journal of Structural and Construction Engineering*. 80(710). 561-570. (in Japanese)

Miyazu, Y. & Soda, S. 2015b. Shake Table Tests on Scaled Three-Story Steel Frames with External Story Drift Control Devices. *Journal of Structural and Construction Engineering*. 80(716). (in press). (in Japanese)

Qu, B., Sanchez-Zamora, F., et al. 2014. Transforming Seismic Performance of Deficient Steel Concentrically Braced Frames through Implementation of Rocking Cores. *Journal of Structural Engineering*. 141(5). 04014139.

Qu, Z., Wada, A., et al. 2012. Pin-supported walls for enhancing the seismic performance of building structures. *Earthquake Engineering and Structural Dynamics*. 41. 2075-2091.

Soda, S. & Yasuda, T. 2007. Effectiveness of Linked Oil Dampers in Seismic Response Control. *Summaries of technical papers of Annual Meeting Architectural Institute of Japan*. B-2. 821-822 (in Japanese).

Takeuchi, T., Chen, X.C., et al. 2014. Seismic Performance of Various Spine Frames with Energy-Dissipation Members. *Journal of Structural and Construction Engineering*. 79(706). 1941-1949 (in Japanese).